HHS Public Access

Author manuscript

Oncogene. Author manuscript; available in PMC 2016 May 18.

Published in final edited form as:

Oncogene. 2016 March 31; 35(13): 1716–1724. doi:10.1038/onc.2015.236.

Endothelial CXCR7 Regulates Breast Cancer Metastasis

Amanda C. Stacer[1], **Joseph Fenner**[1], **Stephen P. Cavnar**[2], **Annie Xiao**[1], **Shuang Zhao**[3], **S. Laura Chang**[4], **Anna Salomonnson**[1], **Kathryn E. Luker**[1], and **Gary D. Luker**[1,2,5,*]

[1]Department of Radiology, University of Michigan Center for Molecular Imaging

[2]Department of Biomedical Engineering, University of Michigan Medical School and College of Engineering

[3]Department of Radiation Oncology, University of Michigan Medical School and College of Engineering

[4]Department of Chemical Engineering, University of Michigan Medical School and College of Engineering

[5]Department of Microbiology and Immunology, University of Michigan Medical School and College of Engineering

Abstract

Atypical chemokine receptor CXCR7 (ACKR3) functions as a scavenger receptor for chemokine CXCL12, a molecule that promotes multiple steps in tumor growth and metastasis in breast cancer and multiple other malignancies. While normal vascular endothelium expresses low levels of CXCR7, marked upregulation of CXCR7 occurs in tumor vasculature in breast cancer and other tumors. To investigate effects of endothelial CXCR7 in breast cancer, we conditionally deleted this receptor from vascular endothelium of adult mice, generating $CXCR7^{\Delta END/\Delta END}$ animals. $CXCR7^{\Delta END/\Delta END}$ mice appeared phenotypically normal, although these animals exhibited a modest 35 ± 3% increase in plasma CXCL12 as compared with control. Using two different syngeneic, orthotopic tumor implant models of breast cancer, we discovered that $CXCR7^{\Delta END/\Delta END}$ mice had significantly greater local recurrence of cancer following resection, elevated numbers of circulating tumor cells, and more spontaneous metastases. $CXCR7^{\Delta END/\Delta END}$ mice also showed greater experimental metastases following intracardiac injection of cancer cells. These results establish that endothelial CXCR7 limits breast cancer metastasis at multiple steps in the metastatic cascade, advancing understanding of CXCL12 pathways in tumor environments and informing ongoing drug development targeting CXCR7 in cancer.

*Correspondence to G.D.L., University of Michigan Medical School, 109 Zina Pitcher Place, A526 BSRB, Ann Arbor, MI 48109-2200. ; Email: gluker@umich.edu

Author Contributions

ACS, JF, SPC, KS, and GDL performed experiments and analyzed data. KEL contributed new reagents. SZ and SLC performed GSEA analyses. KEL and GDL conceptualized and directed the research. ACS, JF, SPC, and GDL wrote the manuscript.

Competing Interests

The authors have no competing financial interests.

Keywords

chemokine; bioluminescence; imaging; animal model

Introduction

Chemokines, a family of peptides that regulate physiologic trafficking of cells, have emerged as key regulators of metastasis ([1], [2]). Compared with normal tissue, malignant and/or stromal cells upregulate multiple chemokines in primary and metastatic tumors. Chemokine CXCL12 is one of the most prominent regulators of tumor growth and metastasis in breast cancer and greater than 20 other human cancers ([3]). CXCL12 secreted by carcinoma-associated fibroblasts in primary breast cancers increases proliferation and invasion of malignant cells and recruits endothelial progenitor cells for tumor angiogenesis ([4]). These processes collectively contribute to vascular intravasation of cancer cells. CXCL12 in primary breast cancers selects for malignant cells that can home, survive, and proliferate in CXCL12-rich metastatic sites such as bone marrow, lung, and brain ([5], [6]). CXCL12 also confers drug resistance in multiple cancers, limiting eradication of cancer cells and further reducing survival ([3], [7], [8]).

CXCL12 binds to chemokine receptors CXCR4 and CXCR7 (recently designated ACKR3), both of which promote progression of cancer to metastatic disease. While CXCR4 typically correlates with greater metastases and reduced survival in cancers including breast, lung, and prostate, outcomes associated with CXCR7 have been less consistently associated with poor prognosis ([9–11]). Expression of CXCR7 in cancer cells promotes tumor growth and metastasis in mouse models of breast and prostate cancer ([12], [13]). In patients, increased levels of CXCR7 correlate with worse survival in malignancies of the gallbladder and kidney ([14], [15]). However, CXCR7 did not affect outcomes in a study of patients with esophageal cancer, and CXCR7 corresponded with better survival in neuroblastoma and rectal cancer ([16–18]). These discrepancies among effects of CXCR7 on survival suggest context-dependent effects of this receptor on cancer progression, including specific types of cells that express CXCR7.

In addition to malignant cells, CXCR7 is expressed on vascular endothelium under normal and pathologic conditions. CXCR7 critically regulates development of the cardiovascular system in two different animal models. Knocking down CXCR7 in zebrafish embryos prevents formation of intersegmental blood vessels, and mice lacking CXCR7 in all tissues frequently suffer early post-natal mortality due to myocardial degeneration and/or heart valve defects ([12]) ([19], [20]). CXCR7 is expressed highly in vasculature of human cancers, including breast, glioma, and renal ([12], [21], [22]). However, effects of tumor endothelial CXCR7 on tumor progression remain unknown.

We investigated effects of CXCR7 on tumor vasculature in breast cancer, a disease in which this receptor is expressed highly on vascular endothelium in mouse models and primary human breast tumors ([12]). Adult mice lacking endothelial CXCR7 appear phenotypically normal, although they have elevated levels of plasma CXCL12. Using two different syngeneic breast cancer cell lines, we discovered that mice lacking CXCR7 on vascular

endothelium have greater spontaneous metastases from orthotopic tumor implants and experimentally-induced breast cancer metastases. Collectively, these results reveal that CXCR7 on vascular endothelium suppresses progression of breast cancer to metastatic disease.

Results

Deletion of endothelial CXCR7 elevates systemic levels of CXCL12

Since embryonic deletion of CXCR7 from vascular endothelium may cause early post-natal death, we deleted CXCR7 conditionally from endothelium of adult mice using the 5′ endothelial enhancer element from the stem cell leukemia (Scl) locus to drive tamoxifen-inducible Cre (Cre^{ERT}). A previous study established this transgene drives expression of Cre^{ERT} selectively in vascular endothelium ([23]). Treatment with tamoxifen deleted CXCR7 as determined by PCR of tail samples, a well-vascularized tissue used previously to screen for Cre-mediated excision of genes from vascular endothelium ([24], [25]) (Fig S1A). These mice also had reduced expression of CXCR7 on endothelium of the liver, an organ with low level expression of this receptor on blood vessels sinusoidal under basal conditions ([26]) (Fig S1B). We used this tamoxifen protocol to delete CXCR7 from vascular endothelium prior to all tumor studies, generating $CXCR7^{\Delta END/\Delta END}$ mice. Adult $CXCR7^{\Delta END/\Delta END}$ mice appeared phenotypically normal.

CXCR7 is a scavenger receptor for CXCL12, removing this chemokine from the extracellular space and degrading it ([27], [28]). Deleting endothelial CXCR7 significantly elevated basal levels of CXCL12 in plasma ($p < 0.05$) (Fig S2). We could not assess effects of CXCR7 on plasma levels of its second chemokine ligand, CXCL11, because a genetic mutation eliminates expression of this gene in C57BL/6 mice ([19]). Overall, these data show that while endothelial CXCR7 is not essential for survival of adult animals, this receptor does regulate circulating levels of CXCL12.

$CXCR7^{\Delta END/\Delta END}$ mice have greater spontaneous metastases from orthotopic breast tumors

We previously identified CXCR7 on tumor blood vessels in mouse xenograft models of breast cancer and primary human breast tumors, while this receptor was absent from vasculature in normal breast tissue ([12]). To investigate effects of endothelial CXCR7 on growth and metastasis in breast cancer, we used AT-3 breast cancer cells, a C57BL/6 mouse breast cancer cell line that expresses modest levels of cell surface CXCR4 and low amounts of CXCR7 (Fig S3). We implanted AT-3 cells expressing firefly luciferase (AT-3-FL) orthotopically into 4^{th} inguinal mammary fat pads of control and $CXCR7^{\Delta END/\Delta END}$ mice. We also implanted mouse mammary fibroblasts stably expressing CXCL12-α to reproduce secretion of this chemokine by stromal cells in primary human breast cancer ([4]).

Bioluminescence imaging showed significantly greater growth of AT-3-FL breast cancer cells in $CXCR7^{\Delta END/\Delta END}$ mice on days 7–16 after implantation ($p < 0.05$) (Fig 1A). We resected orthotopic tumors ~2 weeks after implantation to simulate treatment of patients with breast cancer and allow time for disseminated tumor cells to form detectable

metastases. Resected tumors from control and CXCR7$^{\Delta END/\Delta END}$ mice appeared similar by standard H&E staining and did not differ in relative vascularity assessed by CD31 (Fig 1B). Tumor blood vessels in control mice demonstrated extensive co-localization of CD31 with CXCR7, consistent with prior studies showing increased expression of CXCR7 on that vascular endothelium in breast cancer and other malignancies (Fig 1B) ([12]). By comparison, endothelial expression of CXCR7 and co-localization with CD31 were markedly diminished in tumors from CXCR7$^{\Delta END/\Delta END}$ mice. Immunofluorescence also confirmed expression of CXCR7 in AT-3-FL cells in the tumor.

After resecting orthotopic tumors, we monitored mice for three more weeks for local recurrence and metastases before euthanizing mice on the same day. CXCR7$^{\Delta END/\Delta END}$ mice had significantly larger recurrent tumors in the mammary fat pad and greater overall systemic metastases quantified by bioluminescence (Fig 2A–C). When we analyzed by distribution of metastases in various anatomic sites, CXCR7$^{\Delta END/\Delta END}$ mice had greater metastatic AT-3-FL cells in all locations, although differences between groups of mice only were significant for the total abdomen (Fig 2D). Fluorescence microscopy of lungs *ex* vivo showed small clusters of metastatic AT-3-FL cells in CXCR7$^{\Delta END/\Delta END}$ mice, while control mice had frequent solitary metastatic breast cancer cells as well as cell clusters (Fig S4). CXCR7$^{\Delta END/\Delta END}$ mice also had more viable, circulating AT-3-FL cells than control animals (Fig S5). Since bone and bone marrow represent the most common sites of disseminated tumor cells and breast cancer metastases ([29]), we also recovered bone marrow from lower extremities of mice. We categorized mice as positive for tumor cells in bone marrow based on *ex vivo* bioluminescence above background levels in five independent experiments. Greater than 30% of CXCR7$^{\Delta END/\Delta END}$ mice had viable disseminated AT-3-FL breast cancer cells in bone marrow as compared with less than 15% of controls (Fig 2E). Overall, these data demonstrate that loss of CXCR7 vascular endothelium results in markedly greater spontaneous breast cancer metastases to multiple sites.

To verify these results with a second breast cancer cell line, we used E0771 breast cancer cells, an estrogen receptor positive C57BL/6 medullary adenocarcinoma ([30]). E0771 cells express low levels of cell surface CXCR7 and no detectable CXCR4 by flow cytometry (Fig S3). We co-implanted E0771-FL cells and mouse mammary fibroblasts secreting CXCL12 into mammary fat pads of control and CXCR7$^{\Delta END/\Delta END}$ mice. Unlike AT-3-FL tumors, imaging data showed no difference in growth of E0771 orthotopic tumors through the time we resected tumors 21 days after implantation (Fig 3A). Immediately after resecting tumors, both cohorts had comparable bioluminescence, but imaging showed significantly greater regrowth of E0771-FL cells in CXCR7$^{\Delta END/\Delta END}$ animals by day 34 ($p < 0.05$) (Fig 3A). CXCR7$^{\Delta END/\Delta END}$ mice also had significantly shorter survival than control mice when we monitored animals until euthanized for humane end points or defined as cancer-free based on lack of bioluminescent signal and palpable tumor at 50 days ($p < 0.01$) (Fig 3B).

In an independent experiment with orthotopic E0771 tumors, we resected tumor implants and then euthanized all mice on the same day to quantify spontaneous metastasis. CXCR7$^{\Delta END/\Delta END}$ mice had significantly greater overall spontaneous metastases ($p < 0.01$) (Fig 4A, B). When analyzed by anatomic location, CXCR7$^{\Delta END/\Delta END}$ mice had more metastases in all body sites, although only differences in abdominal metastases were

significant ($p < 0.05$) (Fig 4C). As described for AT-3-FL implants, we recovered blood and bone marrow from extremities and quantified circulating and disseminated tumor cells by *ex vivo* bioluminescence. Combining data from four independent experiments, 57 ± 8% of CXCR7$^{\Delta END/\Delta END}$ mice had circulating E0771-FL cells, while no control mice had any detectable viable cells. We also identified a significantly higher percentage of CXCR7$^{\Delta END/\Delta END}$ mice with disseminated tumor cells in bone marrow ($p < 0.05$); control mice only had E0771-FL cells in bone marrow in one of four experiments (Fig 4D). Therefore, we established that CXCR7$^{\Delta END/\Delta END}$ mice have greater spontaneous metastases using two different breast cancer cell lines.

CXCR7$^{\Delta END/\Delta END}$ mice have greater experimentally-induced metastases

CXCR7$^{\Delta END/\Delta END}$ mice had greater numbers of circulating tumor cells than control animals using orthotopic implants of either AT-3-FL or E0771-FL cells, respectively. Potentially, greater metastasis in CXCR7$^{\Delta END/\Delta END}$ mice could be due to enhanced ability of malignant cells to move from a mammary tumor into the vasculature and/or capability of cells to survive and proliferate in secondary organs.

To eliminate steps in metastasis through vascular intravasation from a localized tumor, we injected breast cancer cells directly into the left ventricle to produce experimental metastases. After intracardiac injection of AT-3-FL cells, we euthanized all animals 15 days later to quantify metastases. Bioluminescence imaging immediately after euthanization showed significantly greater total burden of AT-3-FL cells in CXCR7$^{\Delta END/\Delta END}$ mice with widespread metastases throughout these animals (Fig 5A, B). We observed significantly greater AT-3-FL cells in multiple organs and tissues, including abdomen, omentum, and liver ($p < 0.05$) (Fig 5C). In a separate experiment, we followed mice for survival after intracardiac injection of AT-3-FL cells instead of euthanizing animals at the same time. CXCR7$^{\Delta END/\Delta END}$ mice had significantly shorter survival with 50% of animals reaching humane endpoints by 18 days ($p < 0.05$) (Fig 5D). By comparison, 50% of control mice survived until day 26. CXCR7$^{\Delta END/\Delta END}$ mice also had significantly greater percentages of mice with disseminated AT-3-FL cells in bone marrow (Fig S6). CXCR7$^{\Delta END/\Delta END}$ mice with intracardiac injection of E0771 cells also showed a trend toward shorter survival than control mice, although differences between groups were not significant (Fig S7). These studies demonstrate that greater metastasis in CXCR7$^{\Delta END/\Delta END}$ mice is not solely due to more intravasation of breast cancer cells from mammary tumors, particularly for AT-3-FL cells that express both CXCR4 and CXCR7.

Discussion

Atypical chemokine receptor CXCR7 (ACKR3) is a prominent component of tumor microenvironments in multiple human cancers. Increased expression of CXCR7 commonly occurs on malignant cells in several different human cancers, including breast, renal, colon, and esophagus ([14–16, 31]). CXCR7 also is expressed by endothelial cells in tumor-associated blood vessels found in primary and metastatic sites ([12, 21, 32]). Studies in animal models typically demonstrate that CXCR7 in cancer cells promotes tumor growth and metastasis ([12, 33, 34]). While small molecule inhibitors of CXCR7 reduce tumor growth

and metastasis in animal models, these systemic agents affect the receptor on both cancer and stromal cells ([35–37]). Therefore, effects of endothelial CXCR7 on cancer progression remain unknown.

To investigate endothelial CXCR7 in cancer, we used a genetically-engineered mouse model to conditionally delete this receptor from vascular endothelium. Cre-mediated excision of endothelial CXCR7 in adult mice had no gross phenotype, unlike peri-natal lethality caused by deleting this receptor from endothelium *in utero* ([19]). Using two different syngeneic breast cancer cell lines, we discovered that mammary tumor implants spontaneously metastasize more extensively in $CXCR7^{\Delta END/\Delta END}$ mice. These mice also had greater metastases following systemic injection of breast cancer cells, which bypasses the vascular intravasation step in metastasis. Effects on metastasis occurred without altering overall $CD31^{+}$ vasculature in mammary tumors, indicating that endothelial CXCR7 is not required for tumor angiogenesis in this model.

Similar to other members of the newly designated family of atypical chemokine receptors, CXCR7 functions in part as a scavenger receptor for CXCL12. In cell-based assays, CXCR7 efficiently removes CXCL12 from the extracellular space and degrades it ([27, 28]). Prior studies demonstrate that CXCR7 also controls amounts of CXCL12 in living organisms ([31, 38]). Plasma CXCL12 increases by approximately 4-6-fold in mice with complete knockout of this receptor from all tissues or treated systemically with an inhibitor of CXCR7. In the current study, selective genetic deletion of CXCR7 only from vascular endothelium elevates plasma CXCL12 by ~35% in mice without breast tumors. This result confirms a recent study by Berahovich et al showing immunodetectable CXCR7 on endothelium of venules in organs including spleen, lung, and kidney, suggesting that endothelial CXCR7 could control systemic levels of CXCL12 ([38]).

Local and systemic increases in CXCL12 produce different outcomes, depending on amounts of CXCL12 and context. In some experimental systems, loss of CXCR7 and associated elevation of CXCL12 cause phenotypes due to reduced levels of cell surface CXCR4. CXCR7 scavenging of CXCL12 establishes chemotactic gradients necessary for migration of lateral line primordial cells in zebrafish and neurons during brain development in mice ([27, 39–42]). For both of these systems, loss of CXCR7 produces persistent, relatively high levels of CXCL12 that cause internalization and degradation of CXCR4 on migrating cells, resulting in loss of chemotaxis. However, we did not observe reduced levels of CXCR4 on natural killer cells in bone marrow of $CXCR7^{\Delta END/\Delta END}$ mice (data not shown), suggesting that modest elevations of CXCL12 in these mice did not affect cell surface expression of CXCR4. We note that a requirement for CXCR7 scavenging in CXCL12-CXCR4 chemotaxis depends on overall levels of this chemokine. Using a microfluidic model of chemotaxis, high levels of CXCL12 produced loss of cell surface CXCR4 and cell migration in the absence of cells with CXCR7, but cells maintained cell surface CXCR4 and migrated toward low levels of CXCL12 even without CXCR7 scavenging ([43]). Reinforcing integrated effects of CXCL12 levels and CXCR7, $CXCR7^{\Delta END/\Delta END}$ mice did not have greater spontaneous breast cancer metastasis without co-implanted fibroblasts to reproduce known secretion of CXCL12 by carcinoma-associated fibroblasts in primary human breast cancer (data not shown) ([4, 44]).

Modest elevations of plasma CXCL12 in CXCR7$^{\Delta END/\Delta END}$ mice may be more consistent with conditions that maintain CXCR4 signaling to promote tumor progression and metastasis. The ~35% increase in CXCL12 in CXCR7$^{\Delta END/\Delta END}$ mice is similar to the 14% increase in systemic CXCL12 reported for patients with breast cancer ([45]). In this clinical study, progressive increases in CXCL12 correlated with established markers of poor prognosis, including high grade tumors and basal subtype, suggesting that our mouse model may reproduce effects of moderately elevated CXCL12 on patient outcomes.

CXCL12 regulates multiple steps in tumor growth and metastasis, many of which increased in CXCR7$^{\Delta END/\Delta END}$ mice. In both AT-3 and E0771 orthotopic mammary tumor models, deletion of endothelial CXCR7 increased circulating tumor cells, suggesting greater vascular intravasation of breast cancer cells and/or survival in the circulation. CXCR4 and CXCR7 promote cell migration through tissues and resistance to anoikis, processes that would increase circulating tumor cells ([6, 46–48]). CXCR7$^{\Delta END/\Delta END}$ mice had greater local recurrence and spontaneous metastasis to multiple organs including bone marrow, one of the most common sites of metastatic breast cancer cells in patients. Greater spontaneous metastases in CXCR7$^{\Delta END/\Delta END}$ mice indicates that elevated CXCL12 may promote trafficking of circulating tumor cells to CXCL12-rich organs, enhance survival of disseminated tumor cells in secondary sites, and/or increase proliferation to produce overt metastases. Increases in growth of breast cancer cells after implantation into mammary fat pads were more pronounced with AT-3 cells. We note that AT-3 cells express cell surface CXCR4 and CXCR7, while flow cytometry showed only CXCR7 in E0771. The difference in initial growth of breast cancer cells in mammary fat pads suggests that CXCL12 signaling through CXCR4 is more important for this step in tumor progression. Similarly, when we bypassed the vascular intravasation step by injecting breast cancer cells systemically, we also determined that only CXCR7$^{\Delta END/\Delta END}$ mice with AT-3 cells had significantly shorter survival. This result suggests that CXCL12-CXCR7 interactions on cancer cells may promote intravasation in the mammary tumor environment, which is consistent with a prior cell culture study demonstrating that CXCR7 functions in transendothelial migration of cells ([46]).

To nominate other potential mechanisms through which endothelial CXCR7 may regulate affect breast cancer, we performed a bioinformatics analysis of the TCGA breast cancer data base. While we recognize that the TCGA does not segregate expression data by cell type, endothelial cells in almost all breast cancers express CXCR7. GSEA revealed that CXCR7 correlates negatively with proliferation in comparison with 4 of 5 data sets, suggesting that loss of endothelial CXCR7 in tumor environments may increase proliferation of breast cancer cells in primary tumors and/or metastases (Fig S8). In some contexts, endothelial CXCR7 may increase influx of immune cells into organs and tissues, suggesting potential effects on tumor immunity and regulation of metastasis by immune cells ([49, 50]).

While CXCR7 has been reported to increase proliferation of endothelial cells in vitro, this receptor was not essential for tumor angiogenesis in our mouse model as assessed by CD31 staining of mammary tumors ([51]) ([52]). This discordance likely reflects the large number of cytokines and chemokines that control angiogenesis in living systems, providing redundancy that compensates for loss of a single molecule. Such redundancy has been evident in

resistance to therapies targeting a single regulator of tumor angiogenesis ([53]). Previous studies demonstrate that other tumor endothelial markers do not necessarily decrease tumor angiogenesis, showing our results are not unique to CXCR7 in tumor vasculature ([54, 55]). Further studies are planned to establish functions of endothelial CXCR7 in other types of cancer and different diseases.

Overall, we determined that CXCR7$^{\Delta END/\Delta END}$ mice have modestly elevated systemic levels of CXCL12, showing that endothelial CXCR7 contributes to overall regulation of this chemokine *in vivo*. Deletion of endothelial CXCR7 results in greater spontaneous and experimentally-induced breast cancer metastasis, indicating that vascular CXCR7 suppresses processes including tumor growth, vascular intravasation, and survival and proliferation of breast cancer cells in multiple organs and tissues. These data advance our understanding of CXCR7 and emphasize tissue context-dependent functions of this receptor in cancer. We note that in some experimental systems, pharmacologic inhibition of a molecular target may produce different outcomes than genetic deletion in adult animals ([56, 57]). However, our results suggest that targeting small molecule inhibitors of CXCR7 selectively to cancer cells, such as with nanoparticles, may improve therapeutic benefits by blocking oncogenic functions of this receptor on malignant cells while maintaining effects of endothelial CXCR7 to limit tumor progression.

Materials and Methods

Cells

C57BL/6 mouse breast cancer cell lines AT-3 and E0771 (gifts of Dr. Abrams and Dr. Mihich, Roswell Park Cancer Institute) were cultured in DMEM with 10% fetal bovine serum and 1% glutamine/penicillin/streptomycin (Life Technologies, Carlsbad, CA). We also cultured immortalized mammary fibroblasts from C57BL/6 mice (gift of Dr. Moses, Vanderbilt University) in the same medium. We cultured all cells at 37°C with 5% CO_2.

Lentiviruses

We stably transduced mouse mammary fibroblasts with CXCL12-α fused to fluorescent protein mCherry (MMF-CXCL12) and breast cancer cells with firefly luciferase (AT-3-FL and E0771-FL, respectively) as described ([58, 59]).

Mice

The University of Michigan Committee for Care and Use of Animals approved all mouse procedures. We crossed mice with CXCR7 flanked by LoxP sites (gift of ChemoCentryx) with transgenic mice carrying tamoxifen-inducible Cre-ER^T recombinase under control of the stem cell leukemia (*Scl*) stem cell enhancer (gift of Dr. Begley and the University of Western Australia) for endothelial-specific expression ([23, 26]). We backcrossed mice 12 generations on a C57BL/6 background.

To activate Cre, we treated mice every other day for seven days with 5 mg/kg taxmoxifen (Sigma, St. Louis, MO) in corn oil by intraperitoneal injection. We treated control mice with vehicle only. We also performed selected experiments with Cre-negative mice treated with

tamoxifen rather than vehicle only and obtained similar results. We verified deletion of CXCR7 by PCR of tail biopsies. Since mouse tail tissue is well-vascularized, this strategy has been used previously to verify Cre-mediated deletion of a target gene from endothelium ([24], [25]). PCR primers for genotyping are shown in Table 1.

Mouse tumor model

We established orthotopic tumors by implanting 2×10^5 breast cancer cells (E0771-FL or AT-3-FL) with 1×10^5 MMF-CXCL12 cells in 4th inguinal mammary fat pads of age-matched, 5–8 week old female CXCR7$^{\Delta END/\Delta END}$ or littermate control mice (n = 8–12 per group with specific numbers for each experiment listed in figure legends). These samples sizes are based on prior experience with imaging and disease progression studies in mice. Mice were assigned to groups based on genotype, and investigators knew the genotype of experimental groups. To generate systemic metastases, we injected 1×10^5 breast cancer cells directly into the left ventricle of the heart (n = 8–10 per group as listed in figure legends). We used bioluminescence imaging (IVIS Spectrum, Perkin-Elmer, Waltham, MA) to measure tumor burden and metastases as described ([60]).

When experiments were terminated for humane reasons, we injected luciferin i.p. prior to euthanizing an animal and then imaged metastases immediately after death ([31]). We quantified metastases based on region-of-interest analysis of bioluminescence for total body, chest, and abdomen. We subdivided the chest region into ribs and lungs, while we defined sub-regions of the abdomen as omentum, liver, and intestines with associated mesenteric lymph nodes. In selected experiments, we collected blood for circulating tumor cells via a 28 gauge needle inserted into the right side of the heart of anesthetized mice immediately before euthanization. We cultured blood samples overnight in DMEM growth medium; washed cells with PBS to remove red blood cells; and then measured firefly luciferase bioluminescence in cancer cells after one week. To detect tumor cells in bone marrow, we flushed each femur and tibia with PBS (1 ml per bone); dissociated bone marrow plugs by repeated pipetting; and then cultured cells in DMEM growth medium for one week. We quantified relative numbers of viable tumor cells in bone marrow by bioluminescence.

ELISA

We measured levels of CXCL12 in plasma by ELISA according to the manufacturer's directions (R&D Systems, Minneapolis, MN).

Immunostaining

We fixed tumors in 4% buffered formalin overnight and then embedded tissues in paraffin for sectioning. To stain CXCR7 in tumor vasculature, we snap froze tumors or livers (Tissue-TEK®, VWR International, Radnor, PA) for subsequent cryosectioning of samples at 8 μm thickness. We stained paraffin sections with hematoxylin and eosin for tumor histology. We identified tumor blood vessels with an antibody to CD31 (eBioscience, San Diego, CA). In selected experiments, we also stained sections with CXCR7 (11G8, gift of ChemoCentryx, Mountain View, CA) to co-localize this receptor to tumor blood vessels ([12]). For immunostaining of CXCR7 with antibody 11G8, we blocked tumor sections with 0.1 mg/ml Fab fragment goat anti-mouse IgG (H+L) (Jackson Immunoresearch, West Grove,

PA) for one hour to prevent background from mouse-on-mouse staining prior to adding primary antibodies. For CD31 staining, we quantified the percent area stained with antibody in four randomly selected 20X microscopic fields using ImageJ ([61]).

Flow cytometry

We analyzed cell surface expression of CXCR4 or CXCR7 on breast cancer cells with fluorescent-conjugated antibodies 12G5 and 11G8, respectively (R&D Systems) ([62]).

GSEA analysis

We performed RNAseq data retrieval and normalization as described previously and then correlated all individual genes to CXCR7 expression in the TCGA breast samples to generate a pre-ranked list based on Spearman's Rho ([63]). To perform Gene Set Enrichment Analysis (GSEA), we used the MsigDB collections C2, C5, and C6 ([64]). We presented findings for gene sets related to proliferation and also performed an unbiased review of the top positively and negatively enriched gene sets to nominate potential mechanisms of action.

Statistical analysis

We performed animal studies 2–5 times with independent cohorts of mice. Graphs present mean values with standard error of the mean (SEM). We analyzed data using one-way ANOVA (GraphPad Prism, San Diego, CA) with $p \leq 0.05$ defining statistically significant differences.

Supplementary Material

Refer to Web version on PubMed Central for supplementary material.

Acknowledgments

The authors thank Dr. Mark Penfold and ChemoCentryx for CXCR7 loxP mice and antibody 11G8. Dr. Jun-Lin Guan provided SCL Cre^{ERT} through courteous permission of Dr. Glenn Begley. We thank Dr. Aaron Robida from the University of Michigan Flow Cytometry Core for assistance. Research was supported by United States National Institute of Health grants R21CA182333, R01CA136553, R01CA142750, R01CA170198, and P50CA093990.

References

1. Balkwill F. Cancer and the chemokine network. Nat Rev Cancer. 2004; 4(7):540–50. [PubMed: 15229479]
2. Ali S, Lazennec G. Chemokines: novel targets for breast cancer metastasis. Cancer Metastasis Rev. 2007; 26(3–4):401–20. [PubMed: 17717637]
3. Teicher B, Fricker S. CXCL12 (SDF-1)/CXCR4 pathway in cancer. Clin Cancer Res. 2010; 16(11): 2927–31. [PubMed: 20484021]
4. Orimo A, Gupta P, Sgroi D, Arenzana-Seisdedos F, Delaunay T, Naeem R, et al. Stromal fibroblasts present in invasive human breast carcinomas promote tumor growth and angiogenesis through elevated SDF-1/CXCL12 secretion. Cell. 2005; 121(3):335–48. [PubMed: 15882617]
5. Zhang X, Jin X, Malladi S, Zou Y, Wen Y, Brogi E, et al. Selection of bone metastasis seeds by mesenchymal signals in the primary tumor stroma. Cell. 2013; 154(5):1060–73. [PubMed: 23993096]
6. Muller A, Homey B, Soto H, Ge N, Catron D, Buchanon M, et al. Involvement of chemokine receptors in breast cancer metastasis. Nature. 2001; 410(6824):50–6. [PubMed: 11242036]

7. Singh S, Srivastava S, Bhardwaj A, Owen L, Singh A. CXCL12-CXCR4 signalling axis confers gemcitabine resistance to pancreatic cancer cells: a novel target for therapy. Br J Cancer. 2010; 103(11):1671–9. [PubMed: 21045835]
8. Hoellenriegel J, Zboralski D, Maasch C, Rosin N, Wierda W, Keating M, et al. The Spiegelmer NOX-A12, a novel CXCL12 inhibitor, interferes with chronic lymphocytic leukemia cell motility and causes chemosensitization. Blood. 2014; 123(7):1032–9. [PubMed: 24277076]
9. Akashi T, Koizumi K, Tsuneyama K, Saiki I, Takano Y, Fuse H. Chemokine receptor CXCR4 expression and prognosis in patients with metastatic prostate cancer. Cancer Sci. 2008; 99(3):539–42. [PubMed: 18201276]
10. Xu T, Shen H, Liu L, Shu Y. The impact of chemokine receptor CXCR4 on breast cancer prognosis: a meta-analysis. Cancer Epidemiol. 2013; 37(5):725–31. [PubMed: 23763828]
11. Wald O, Shapira O, Izhar U. CXCR4/CXCL12 axis in non small cell lung cancer (NSCLC) pathologic roles and therapeutic potential. Theranostics. 2013; 3(1):26–33. [PubMed: 23382783]
12. Miao Z, Luker K, Summers B, Berahovich R, Bhojani M, Rehemtulla A, et al. CXCR7 (RDC1) promotes breast and lung tumor growth in vivo and is expressed on tumor-associated vasculature. Proc Natl Acad Sci U S A. 2007; 104(40):15735–40. [PubMed: 17898181]
13. Wang J, Shiozawa Y, Wang J, Wang Y, Jung Y, Pienta K, et al. The role of CXCR7/RDC1 as a chemokine receptor for CXCL12/SDF-1 in prostate cancer. J Biol Chem. 2008; 283(7):4283–94. [PubMed: 18057003]
14. Yao X, Zhou L, Han S, Chen Y. High expression of CXCR4 and CXCR7 predicts poor survival in gallbladder cancer. J Int Med Res. 2011; 39(4):1253–64. [PubMed: 21986127]
15. D'Alterio C, Consales C, Polimeno M, Franco R, Cindolo L, Portella L, et al. Concomitant CXCR4 and CXCR7 expression predicts poor prognosis in renal cancer. Curr Cancer Drug Targets. 2010; 10(7):772–81. [PubMed: 20578990]
16. Tachezy M, Zander H, Gebauer F, von Loga K, Pantel K, Izbicki J, et al. CXCR7 expression in esophageal cancer. J Transl Med. 2013; 11:238. [PubMed: 24074251]
17. Liberman J, Sartelet H, Flahaut M, Muhlethaler-Mottet A, Coulon A, Nyalendo C, et al. Involvement of the CXCR7/CXCR4/CXCL12 axis in the malignant progression of human neuroblastoma. PLoS One. 2012; 7(8):e43665. [PubMed: 22916293]
18. D'Alterio C, Avallone A, Tatangelo F, Delrio P, Pecori B, Cella L, et al. A prognostic model comprising pT stage, N status and the chemokine receptors CXCR4 and CXCR7 powerfully predicts outcome in neo-adjuvant resistant rectal cancer patients. Int J Cancer. 2013; 135(2):379–90. [PubMed: 24375277]
19. Sierro F, Biben C, Martinez-Munoz L, Mellado M, Ransohoff R, Li M, et al. Disrupted cardiac development but normal hematopoiesis in mice deficient in the second CXCL12/SDF-1 receptor, CXCR7. Proc Natl Acad Sci U S A. 2007; 104(37):14759–64. [PubMed: 17804806]
20. Gerrits H, van Ingen Schenau D, Bakker N, van Disseldorp A, Strik A, Hermens L, et al. Early postnatal lethality and cardiovascular defects in CXCR7-deficient mice. Genesis. 2008; 46(5):235–45. [PubMed: 18442043]
21. Madden S, Cook B, Nacht M, Weber W, Callahan M, Jiang Y, et al. Vascular gene expression in nonneoplastic and malignant brain. Am J Pathol. 2004; 165(2):601–8. [PubMed: 15277233]
22. Maishi N, Ohga N, Hida Y, Akiyama K, Kitayama K, Osawa T, et al. CXCR7: a novel tumor endothelial marker in renal cell carcinoma. Pathol Int. 2012; 62(5):309–17. [PubMed: 22524658]
23. Gőthert J, Gustin S, Hall M, Green A, Gőttgens B, Izon D, et al. In vivo fate-tracing studies using the *Scl* stem cell enhancer: embryonic hematopoietic stem cells significantly contribute to adult hematopoiesis. Blood. 2005; 105(7):2724–32. [PubMed: 15598809]
24. Liao Y, Day K, Damon D, Duling B. Endothelial cell-specific knockout of connexin 43 causes hypotension and bradycardia in mice. Proc Natl Acad Sci USA. 2001; 98(17):9989–94. [PubMed: 11481448]
25. Suárez Y, Fernández-Hernando C, Yu J, Gerber S, Harrison K, Pober J, et al. Dicer-dependent endothelial microRNAs are necessary for postnatal angiogenesis. Proc Natl Acad Sci USA. 2008; 105(37):14082–7. [PubMed: 18779589]

26. Ding B-S, Cao Z, Lis R, Nolan D, Guo P, Simons M, et al. Divergent angiocrine signals from vascular niche balance liver regeneration and fibrosis. Nature. 2013; 505(7481):97–102. [PubMed: 24256728]
27. Boldajipour B, Mahabaleshwar S, Kardash E, Reichman-Fried M, Blaser H, Minina S, et al. Control of chemokine-guided cell migration by ligand sequestration. Cell. 2008; 132(3):463–73. [PubMed: 18267076]
28. Luker K, Steele J, Mihalko L, Luker G. Constitutive and chemokine-dependent internalization and recycling of CXCR7 in breast cancer cells to degrade chemokine ligands. Oncogene. 2010; 29:4599–610. [PubMed: 20531309]
29. Coleman R. Clinical features of metastatic bone disease and risk of skeletal morbidity. Clin Cancer Res. 2006; 12(20 Pt 2):6243s–9s. [PubMed: 17062708]
30. Ewens A, Mihich E, Ehrke M. Distant metastasis from subcutaneously grown E0771 medullary breast adenocarcinoma. Anticancer Res. 2005; 25(6B):3905–15. [PubMed: 16312045]
31. Luker K, Lewin S, Mihalko L, Schmidt B, Winkler J, Coggins N, et al. Scavenging of CXCL12 by CXCR7 regulates tumor growth and metastasis of CXCR4-positive breast cancer cells. Oncogene. 2012; 31(45):4570–8.
32. Guillemot E, Karimdjee-Soilhi B, Pradelli E, Benchetrit M, Goquet-Surmenian E, Millet M, et al. CXCR7 receptors facilitate the progression of colon carcinoma within lung not within liver. Br J Cancer. 2012; 107(12):1944–9. [PubMed: 23169289]
33. Dang S, Peng Y, Ye L, Wang Y, Qian Z, Chen Y, et al. Stimulation of TLR4 by LMW-HA induces metastasis in human papillary thyroid carcinoma through CXCR7. Clin Dev Immunol. 2013; 2013:712561. [PubMed: 24363762]
34. Xue T, Chen R, Han D, Chen J, Xue Q, Gao D, et al. Down-regulation of CXCR7 inhibits the growth and lung metastasis of human hepatocellular carcinoma cells with highly metastatic potential. Exp Ther Med. 2012; 3(1):117–23. [PubMed: 22969855]
35. Burns J, Summers B, Wang Y, Melikian A, Berahovich R, Miao Z, et al. A novel chemokine receptor for SDF-1 and I-TAC involved in cell survival, cell adhesion, and tumor development. J Exp Med. 2006; 203(9):2201–13. [PubMed: 16940167]
36. Goquet-Surmenian E, Richard-Fiardo P, Guillemot E, Benchetrit M, Gomez-Brouchet A, Buzzo P, et al. CXCR7-mediated progression of osteosarcoma in the lungs. Br J Cancer. 2013; 109(6):1579–85. [PubMed: 24002596]
37. Walters M, Ebsworth K, Berahovich R, Penfold M, Liu S, Al Omran R, et al. Inhibition of CXCR7 extends survival following irradiation of brain tumours in mice and rats. Br J Cancer. 2014; 110(5): 1179–88. [PubMed: 24423923]
38. Berahovich R, Zabel B, Lewen S, Walters M, Ebsworth K, Wang Y, et al. Endothelial expression of CXCR7 and the regulation of systemic CXCL12 levels. Immunology. 2014; 141(1):111–22. [PubMed: 24116850]
39. Wang Y, Li G, Stanco A, Long J, Crawford D, Potter G, et al. CXCR4 and CXCR7 have distinct functions in regulating interneuron migration. Neuron. 2011; 69(1):61–76. [PubMed: 21220099]
40. Sanchez-Alcaniz J, Haege S, Mueller W, Pla R, Mackay F, Schulz S, et al. Cxcr7 controls neuronal migration by regulating chemokine responsiveness. Neuron. 2011; 69(1):77–90. [PubMed: 21220100]
41. Dona E, Barry J, Valentin G, Quirin C, Khmelinskii A, Kunze A, et al. Directional tissue migration through a self-generated chemokine gradient. Nature. 2013; 503(7475):285–9. [PubMed: 24067609]
42. Venkiteswaran G, Lewellis S, Wang J, Reynolds E, Nicholson C, Knaut H. Generation and Dynamics of an Endogenous, Self-Generated Signaling Gradient across a Migrating Tissue. Cell. 2013; 155(3):674–87. [PubMed: 24119842]
43. Cavnar S, Ray P, Moudgil P, Chang S, Luker K, Linderman J, et al. Microfluidic source-sink model reveals effects of biophysically distinct CXCL12-isoforms in breast cancer chemotaxis. Integr Biol. 2014; 6(5):564–76.
44. Allinen M, R B, Cai L, Brennan C, Lahti-Domerci J, Huang H, et al. Molecular characterization of the tumor microenvironment in breast cancer. Cancer Cell. 2004; 6(1):17–32. [PubMed: 15261139]

45. Potter S, Dwyer R, Curran C, Hennesy E, Harrington K, Griffin D, et al. Systemic chemokine levels in breast cancer patients and their relationship with circulating menstrual hormones. Breast Cancer Res Treat. 2009; 115(2):279–87. [PubMed: 18521742]
46. Zabel B, Wang Y, Lewen S, Berahovich R, Penfold M, Zhang P, et al. Elucidation of CXCR7-mediated signaling events and inhibition of CXCR4-mediated tumor cell transendothelial migration by CXCR7 ligands. J Immunol. 2009; 183(5):3204–11. [PubMed: 19641136]
47. Kochetkova M, Kumar S, McColl S. Chemokine receptors CXCR4 and CCR7 promote metastasis by preventing anoikis in cancer cells. Cell Death Differ. 2009; 16(5):664–73. [PubMed: 19136936]
48. Sun Y, Mao X, Fan C, Liu C, Guo A, Guan S, et al. CXCL12-CXCR4 axis promotes the natural selection of breast cancer cell metastasis. Tumour Biol. 2014; 35(8):7765–73. [PubMed: 24810923]
49. Cruz-Orengo L, Holman D, Dorsey D, Zhou L, Zhang P, Wright M, et al. CXCR7 influences leukocyte entry into the CNS parenchyma by controlling abluminal CXCL12 abundance during autoimmunity. J Exp Med. 2011; 208(2):327–39. [PubMed: 21300915]
50. Kitamura T, Qian B-Z, Pollard J. Immune cell promotion of metastasis. Nat Rev Immunol. 2015; 15:73–86. [PubMed: 25614318]
51. Raggo C, Ruhl R, McAllister S, Koon H, Dezube B, Fruh K, et al. Novel cellular genes essential for transformation of endothelial cells by Kaposi's sarcoma-associated herpesvirus. Cancer Res. 2005; 65(12):5084–95. [PubMed: 15958552]
52. Totonchy J, Osborn J, Botto S, Clepper L, Moses A. Aberrant proliferation in CXCR7+ endothelial cells via degradation of the retinoblastoma protein. PLoS One. 2013; 8(7):e69828. [PubMed: 23894550]
53. Casanovas O, Hicklin D, Bergers G, Hanahan D. Drug resistance by evasion of antiangiogenic targeting of VEGF signaling in late-stage pancreatic islet tumors. Cancer Cell. 2005; 8(4):299–309. [PubMed: 16226705]
54. Nanda A, Karim B, Peng Z, Liu G, Qiu W, Gan C, et al. *Tumor endothelial marker 1 (Tem1)* functions in the growth and progression of abdominal tumors. Proc Natl Acad Sci USA. 2006; 103(9):3351–6. [PubMed: 16492758]
55. Cullen M, Seaman S, Chaudhary A, Yang M, Hilton M, Logsdon D, et al. Host-derived tumor endothelial marker 8 promotes the growth of melanoma. Cancer Res. 2009; 69(15):6021–6. [PubMed: 19622764]
56. Yokoyama K, Ishikawa N, Igarahsi S, Kawano N, Hattori K, Miyazaki T, et al. Discovery of potent CCR4 antagonists: Synthesis and structure-activity relationship study of 2,4-diaminoquinazolines. Bioorg Med Chem. 2008; 16(14):7021–31. [PubMed: 18539035]
57. Walters M, Ebsworth K, Sullivan T, Zhang P, Powers J, Jaen J, et al. CCR9 inhibition does not interfere with the development of immune tolerance to oral antigens. Immunol Lett. 2013; 151(1–2):44–7. [PubMed: 23333353]
58. Smith M, Luker K, Garbow J, Prior J, Jackson E, Piwnica-Worms D, et al. CXCR4 regulates growth of both primary and metastatic breast cancer. Cancer Res. 2004; 64(23):8604–12. [PubMed: 15574767]
59. Ray P, Mihalko L, Coggins N, Moudgil P, Ehrlich A, Luker K, et al. Carboxy-terminus of CXCR7 regulates receptor localization and function. Int J Biochem Cell Biol. 2012; 44(4):669–78. [PubMed: 22300987]
60. Luker G, Pica C, Song J, Luker K, Piwnica-Worms D. Imaging 26S proteasome activity and inhibition in living mice. Nat Med. 2003; 9(7):969–73. [PubMed: 12819780]
61. Fenner J, Stacer A, Winterroth F, Johnson T, Luker K, Luker G. Macroscopic stiffness of breast tumors predicts metastasis. Sci Rep. 2014; 4:5512. [PubMed: 24981707]
62. Salomonnson E, Stacer A, Ehrlich A, Luker K, Luker G. Imaging CXCL12-CXCR4 signaling in ovarian cancer therapy. PLoS One. 2013; 8(1):e51500. [PubMed: 23372646]
63. Zhao S, Chang S, Linderman J, Feng F, Luker G. A comprehensive analysis of CXCL12 isoforms in breast cancer. Transl Onc. 2014 in press.
64. Subramanian A, Tamayo P, Mootha V, Mukherjee S, Ebert B, Gillette M, et al. Gene set enrichment analysis: A knowledge-based approach for interpreting genome-wide expression profiles. Proc Natl Acad Sci USA. 2005; 102(43):15545–50. [PubMed: 16199517]

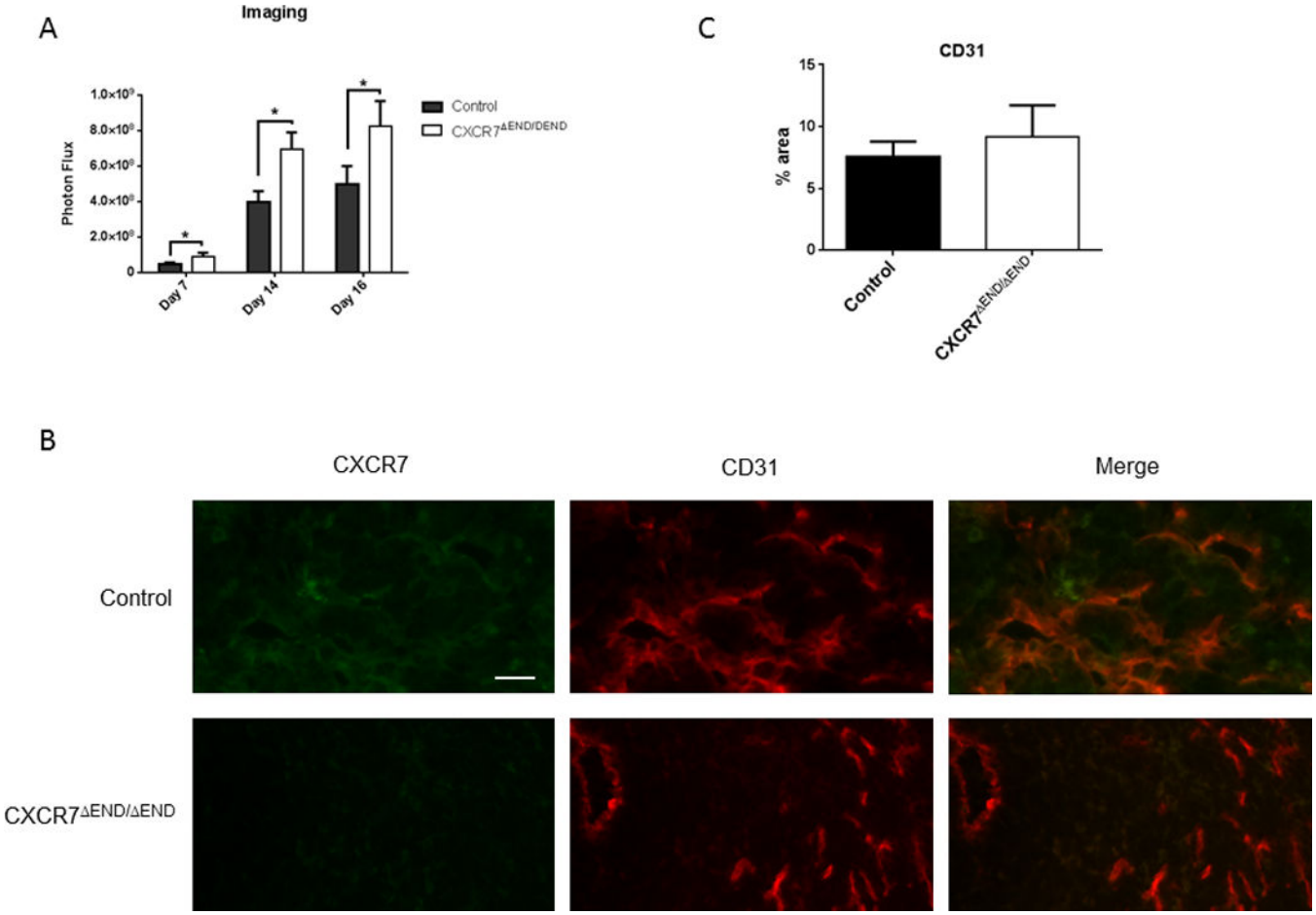

Figure 1. Orthotopic AT-3-FL tumor implants in CXCR7$^{\Delta END/\Delta END}$ mice have more viable tumor cells

A) Growth of AT-3-FL breast cancer cells implanted orthotopically into CXCR7$^{\Delta END/\Delta END}$ and control mice monitored by bioluminescence imaging at indicated days (n = 8 mice per group). Graph depicts mean values + SEM for photon flux. *, $p < 0.05$. B) Immunofluorescence of excised orthotopic AT-3-FL tumors for CD31-tumor vasculature (green) and CXCR7 (red). White arrows show co-localization of CD31 and CXCR7 in merged images. AT-3-FL cells express CXCR7, accounting for staining throughout both tumors. Scale bar designates 50 μm. C. Graph shows mean values + SEM for area occupied by CD31+ blood vessels in tumors from each group of mice.

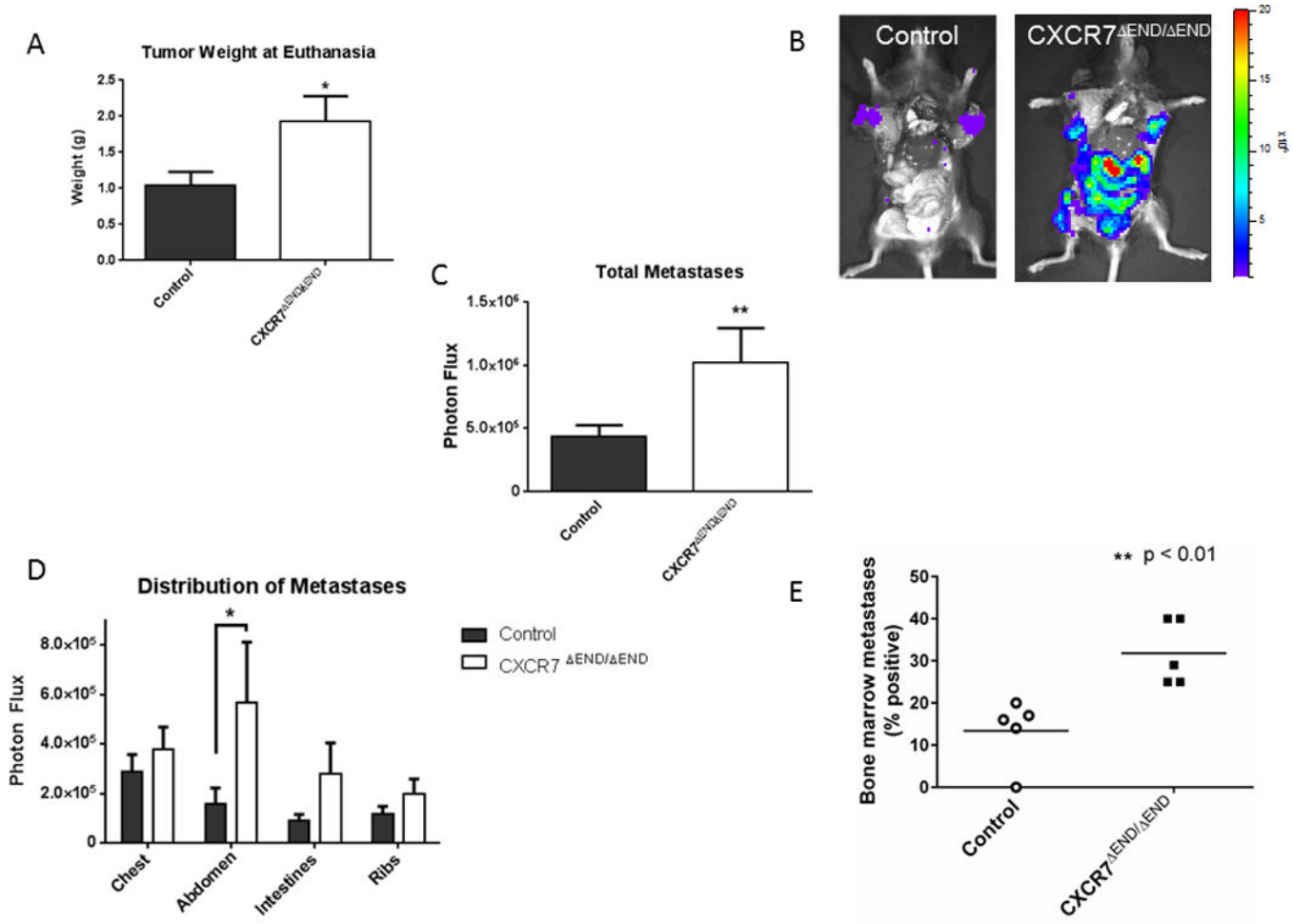

Figure 2. Increased local tumor recurrence and metastases in CXCR7$^{\Delta END/\Delta END}$ mice

A) We resected recurrent tumors from mammary fat pads of CXCR7$^{\Delta END/\Delta END}$ and control mice at the time of euthanization. Weights of recurrent tumors are shown as mean values + SEM (n = 8 mice per group). B) Representative bioluminescence images of metastases in CXCR7$^{\Delta END/\Delta END}$ and control mice immediately after euthanization. C) We quantified total photon flux from AT-3-FL metastases in both groups of mice and graphed data as mean values + SEM. D) Graph shows mean values + SEM for bioluminescent metastases quantified at defined anatomic sites. E) We measured disseminated AT-3-FL cells recovered from bone marrrow of CXCR7$^{\Delta END/\Delta END}$ and control mice by *ex vivo* bioluminescence imaging and determined the percentage of mice in each group with detectable signal above background. Each data point shows percent of mice per group with disseminated tumor cells in bone marrow from five independent experiments (n = 8–10 mice per group per experiment). Horizontal line denotes the mean for each group. *, $p < 0.05$; **, $p < 0.01$.

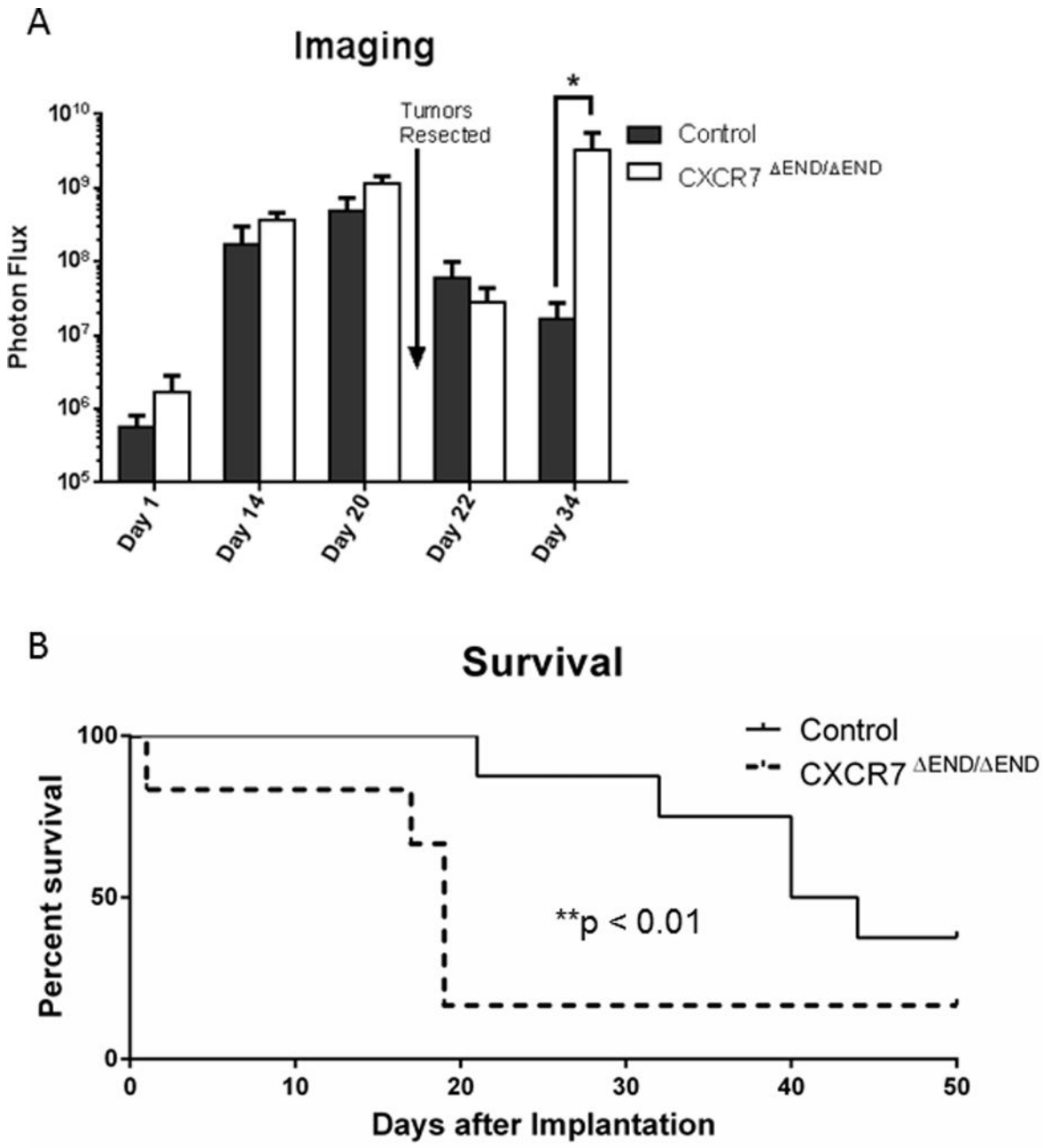

Figure 3. Reduced survival of CXCR7$^{\Delta END/\Delta END}$ mice with orthotopic tumor implants of E0771-FL breast cancer cells

A) We measured tumor growth in mice with orthotopic implants of E0771-FL cells by bioluminescence imaging at indicated days. Graph shows mean values + SEM for photon flux in CXCR7$^{\Delta END/\Delta END}$ and control mice (n = 8 mice per group). Arrow designates when tumor implants were resected on day 21. B) Following resection of orthotopic tumor implants, we monitored CXCR7$^{\Delta END/\Delta END}$ and control mice until each animal had to be euthanized for humane end points. Mice surviving through 50 days had no detectable tumor as assessed by palpation of mammary fat pads and bioluminescence imaging. *, $p < 0.05$.

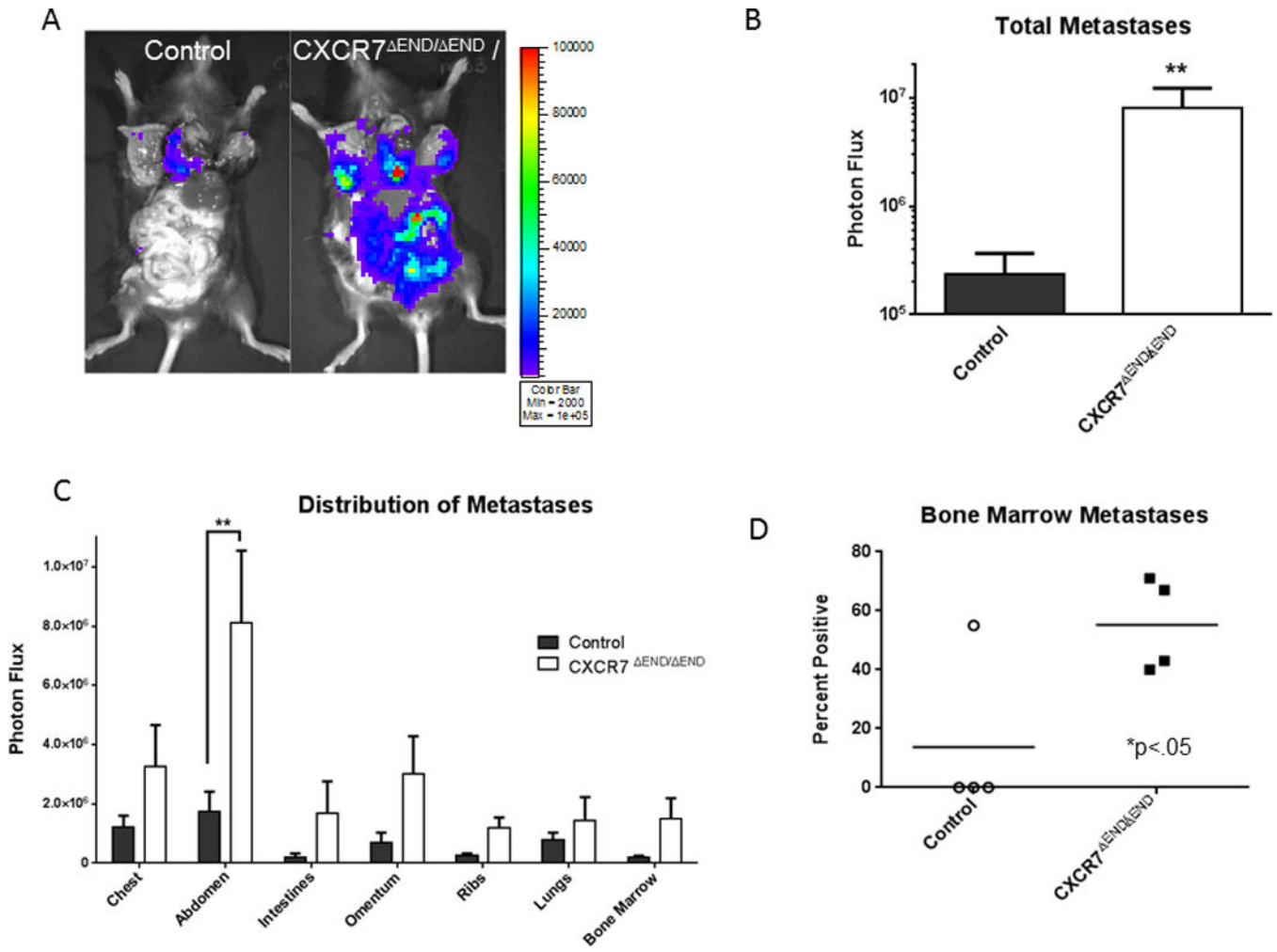

Figure 4. CXCR7$^{\Delta END/\Delta END}$ mice with orthotopic E0771-FL tumors have greater spontaneous metastases

A) Representative bioluminescence images of metastatic E0771-FL cells in euthanized CXCR7$^{\Delta END/\Delta END}$ and control mice. B) Graph of total metastases measured in euthanized mice presented as mean values + SEM (n = 8 per group). C) Anatomic distribution of metastasis quantified by bioluminescence imaging of mice immediately after euthanization. Data are presented as mean values + SEM. D) We quantified disseminated E0771-FL cells in bone marrow by *ex vivo* bioluminescence imaging. Each point shows the percentage of CXCR7$^{\Delta END/\Delta END}$ and control mice with detectable breast cancer cells in bone marrow in a given experiment (n = 8–10 mice per group per experiment). Horizontal line shows mean values for percent mice with disseminated tumor cells in four independent experiments. **, $p < 0.01$.

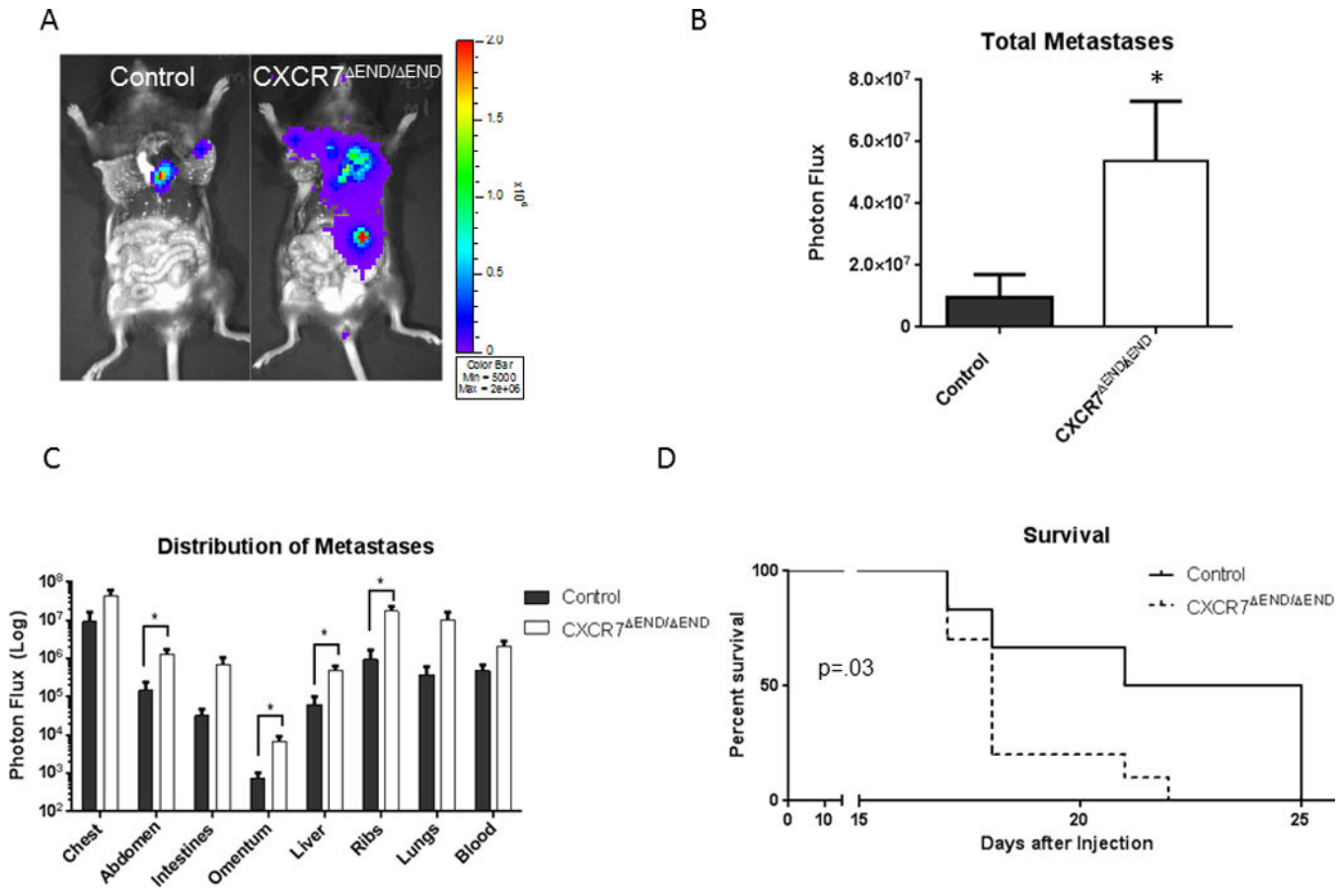

Figure 5. AT-3-FL cells produce greater experimental metastases in CXCR7$^{\Delta END/\Delta END}$ mice

A) We injected AT-3-FL cells systemically via injection into left ventricles of CXCR7$^{\Delta END/\Delta END}$ and control mice. Presented images are representative of relative amounts of metastatic AT-3-FL cells at the time of euthanization. B) We quantified total AT-3-FL metastases by bioluminescence imaging and graphed data as mean values + SEM for each group (n = 12 each). C) We determined site-specific localization of metastases by bioluminescence imaging and quantified tumor burden as mean values + SEM for photon flux in each site. D) Survival curves for a separate experiment in which AT-3-FL cells were injected into CXCR7$^{\Delta END/\Delta END}$ and control mice and monitored until animals were euthanized for humane endpoints (n = 12 per group). * $p < 0.05$.

Table 1

PCR primers for analyzing mice.

Cre	forward	TCGATGCAACGAGTGATGAG
	reverse	TTCGGCTATACGTAACAGGG
LoxP flanked CXCR7	forward	CTACAGCTTCATCAACCGCAAC
	reverse	GTCCTGGRGCTGGCTTTGAT
CXCR7 deletion	forward	GCAAGTTTGGGGTACAGTCC
	reverse	GAGAGACAGGAAGCATGGTCAC